

1 **Enrichment of ammonium in the future ocean threatens diatom productivity**

2 **Pearse J. Buchanan^{1,2,3}, Juan J. Pierella Karlusich^{4,5}, Robyn E. Tuerena⁶, Roxana Shafiee⁷,**
3 **E. Malcolm S. Woodward⁸, Chris Bowler⁵, and Alessandro Tagliabue².**

4 ¹CSIRO Environment, Hobart, 7004, Australia.

5 ²Department of Earth, Ocean and Ecological Sciences, University of Liverpool; Liverpool, L69
6 3GP, UK.

7 ³Department of Global Ecology, Carnegie Institution for Science; Stanford, CA, 94305, USA.

8 ⁴FAS Division of Science, Harvard University, Cambridge, MA, 02138, USA.

9 ⁵Institut de Biologie de l'École Normale Supérieure, Département de Biologie, École Normale
10 Supérieure, CNRS, INSERM, Université de Recherche Paris Sciences et Lettres, Paris, France.

11 ⁶Scottish Association for Marine Science; Dunstaffnage, Oban, PA37 1QA, UK.

12 ⁷Center for the Environment, Harvard University, Cambridge, MA, 02138.

13 ⁸Plymouth Marine Laboratory; Plymouth, PL1 3DH, UK.

14
15 Corresponding author: Pearse J Buchanan (pearse.buchanan@csiro.au)
16

17 **Key Points:**

- 18 • An ocean biogeochemical model shows an enrichment in ammonium relative to total
19 nitrogen in over 98% of the surface ocean.
- 20 • *Tara* Oceans data reveals a global negative relationship between diatoms and ammonium
21 to total nitrogen ratios.
- 22 • We attribute 70% of future losses in diatom relative abundance in marine ecosystems to
23 ammonium enrichment.

24 **Abstract**

25 Diatoms are prominent eukaryotic photoautotrophs in today's oceans. While dominant in nitrate-
26 rich conditions, they face competitive exclusion by other phytoplankton when ammonium forms
27 the bulk of bioavailable nitrogen. The extent to which this competitive exclusion defines diatom
28 abundance worldwide and the consequences of potential future ammonium enrichment remain
29 unexplored and unquantified. Here, using phytoplankton abundance proxies from the *Tara*
30 Oceans dataset and an ocean-biogeochemical model, we demonstrate that ammonium enrichment
31 reduces diatom prevalence in marine ecosystems at the global-scale. Under a high emission
32 scenario, we anticipate 98% of the euphotic zones to experience ammonium enrichment by 2081-
33 2100 and attribute a majority (70%) of future diatom displacement to competitive exclusion by
34 other phytoplankton as bioavailable nitrogen supply shifts from nitrate to ammonium. Overall,
35 the form of nitrogen emerges as a significant but previously underestimated stressor affecting
36 diatoms and ocean ecosystems globally.

37

38 **Plain Language Summary**

39 This work investigates how a type of microscopic algae called diatoms are affected by changes
40 in the form of nitrogen that is available in the sunlit surface ocean. Diatoms are crucial for ocean
41 health and carbon cycling because they grow and sink rapidly. Diatoms typically thrive in waters
42 with high concentrations of nitrate, an oxidized form of nitrogen, but they are outcompeted by
43 other algae when ammonium, a reduced form, is the primary source of nitrogen. We use both
44 observations and modelling to understand how a widespread future enrichment of ammonium
45 within marine ecosystems might affect diatom relative abundance. We attribute that the
46 enrichment of ammonium can explain 70% of the projected losses to diatom relative abundance
47 by the end of the 21st century if greenhouse gas emissions continue unabated. The form of
48 nitrogen, whether oxidized or reduced, is thus an important control on diatom relative
49 abundance.

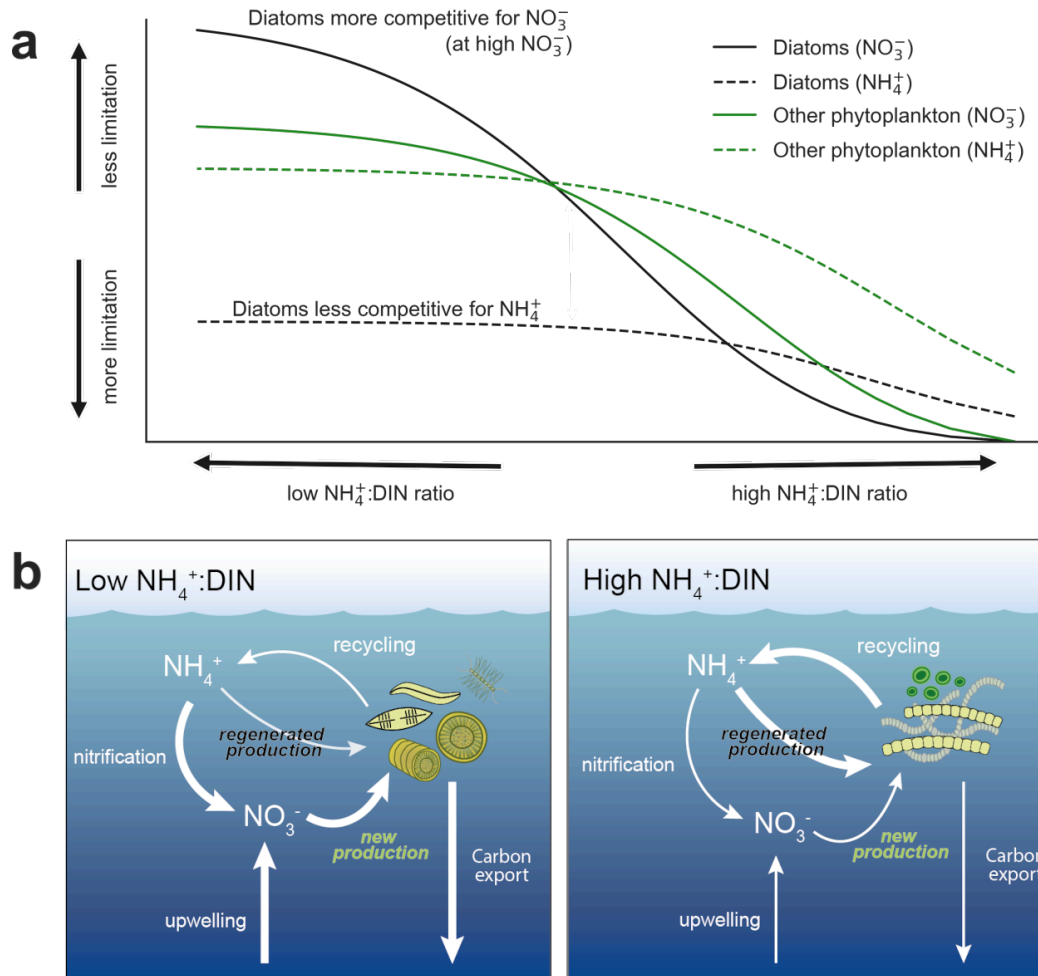
50

51 **1 Introduction**

52 Diatoms are among the most successful and diversified eukaryotic photoautotrophs in the
53 present-day ocean (Armbrust, 2009; Pierella Karlusich et al., 2020). Part of their success is due
54 to their competitive edge for growth on nitrate (NO_3^-) as a source of bioavailable nitrogen (Berg
55 et al., 2003; Carter et al., 2005; Donald et al., 2013; Fawcett et al., 2011; Glibert et al., 2016;
56 Klawonn et al., 2019; Litchman, 2007; Van Oostende et al., 2017; Selph et al., 2021; Tungaraza
57 et al., 2003; Xianhui Sean Wan et al., 2018), which also underpins their role as
58 disproportionately large contributors to “new” (NO_3^- -fueled) primary production (Fawcett et al.,
59 2011). As new production is linked to the rate of organic carbon export to the ocean interior
60 (Dugdale & Goering, 1967), diatoms also contribute significantly to oceanic carbon dioxide
61 sequestration and the ocean's most productive fisheries (Cushing, 1989; Legendre, 1990;

62 Tréguer et al., 2018). However, this apparent preference for NO_3^- may instead reflect that they
63 are competitively excluded by other phytoplankton when the primary substrate for growth is
64 ammonium (NH_4^+). While diatoms tend to have a higher affinity for NO_3^- than other
65 phytoplankton, making them adept competitors for NO_3^- when NO_3^- is the primary nitrogen
66 substrate, investigations into the kinetics of nutrient uptake have identified that diatoms have a
67 lower affinity for NH_4^+ than other major groups of phytoplankton (Litchman et al., 2007) (Fig.
68 1a). Their low affinity for NH_4^+ means that diatoms tend to be competitively excluded by other
69 phytoplankton taxa, such as the smaller (although not always (Arsenieff et al., 2020; Leblanc et
70 al., 2018; Pierella Karlusich et al., 2020)) cyanobacteria and green algae, when nitrogen is
71 limiting and NH_4^+ is the dominant source of nitrogen (Litchman et al., 2007).

72 Variations in circulation and biogeochemical processes control the form of nitrogen that supports
73 primary production in the sunlit upper ocean (Fig. 1b). As mixing injects NO_3^- from deeper
74 waters, it becomes the dominant form in areas of upwelling, especially when limitation by iron,
75 light or grazing pressure slows uptake by phytoplankton. In stratified systems, NH_4^+ and other
76 forms of reduced nitrogen (e.g., urea and other organics, which can be important nitrogen
77 sources (Morando & Capone, 2018)) dominate the bioavailable nitrogen pool. Nitrate supply is
78 restricted by a lack of vertical mixing, consequently depleted, and demand is instead satisfied by
79 NH_4^+ through an intense heterotrophic recycling of organic matter. Although nutrient stocks are
80 low, the rapidity of this recycling supports net autotrophy and “normal” rates of primary
81 production as measured via carbon uptake incubations and isotopes in the subtropical gyres
82 (Bender & Jönsson, 2016; Matsumoto et al., 2016; Rii et al., 2016; Yang et al., 2019). Intense
83 competition for NH_4^+ in these environments not only excludes the less competitive
84 phytoplankton species, but also the archaea and bacteria that are responsible for ammonia
85 oxidation, which would otherwise resupply nitrite and nitrate and alter the form of nitrogen
86 available for growth (Xianhui Sean Wan et al., 2018; Zakem et al., 2018). Thus, while nitrogen
87 concentrations are low in stratified systems, there is intense competition for a rapid supply of
88 NH_4^+ .



89

90 **Fig. 1. Competitive outcomes for phytoplankton dependent on regimes of nitrogen cycling**
 91 **in the upper ocean.** (a), Example limitation of diatoms (black) and other generic phytoplankton
 92 (green) by nitrate (solid lines) and ammonium (dashed lines) as a function of changing
 93 $\text{NH}_4^+:\text{DIN}$ ratios. $\text{NH}_4^+:\text{DIN}$ ratios (x-axis) are altered by increasing NO_3^- while holding NH_4^+
 94 constant. Diatoms are always more limited by growth on NH_4^+ than other phytoplankton groups.
 95 These limitation functions are integrated within the biogeochemical model. (b), Two regimes of
 96 nitrogen cycling with low and high $\text{NH}_4^+:\text{DIN}$ ratios. Nitrogen in the form of NO_3^- is mixed into
 97 the euphotic zone, taken up by phytoplankton, including diatoms, to produce organic matter (new
 98 production). Organic matter sinks and contributes to carbon export or is consumed by
 99 heterotrophs and recycled to NH_4^+ . NH_4^+ may be nitrified to NO_3^- or consumed by phytoplankton
 100 (regenerated production).

101

102 Ongoing and projected climate change is expected to alter both circulation and biogeochemical
 103 processes and consequently alter the relative availability of NH_4^+ in marine environments.

104 Hereafter, we use the NH_4^+ to dissolved inorganic nitrogen ratio ($\text{NH}_4^+:\text{DIN}$), where $\text{DIN} = \text{NH}_4^+$
105 $+ \text{NO}_2^- + \text{NO}_3^-$, as a measure of this relative availability in the form of nitrogen. When we refer
106 to enrichment of NH_4^+ , we specifically mean an increase in the amount of DIN that is NH_4^+ , with
107 an enrichment consistent with a higher proportion of primary production supported through
108 regeneration (i.e., NH_4^+ -based). Physical changes, including a changing oceanic circulation
109 (Sallée et al., 2021), is expected to limit inputs of NO_3^- from deeper waters to further intensify
110 nitrogen limitation of phytoplankton communities (Bopp et al., 2005; Buchanan et al., 2021).
111 Climate warming is expected to accelerate the metabolism of phytoplankton (Eppley, 1972) and
112 thereby increase nitrogen demand and recycling rates (Cherabier & Ferrière, 2022). Meanwhile,
113 ocean acidification may decelerate rates of microbial ammonia oxidation (Beman et al., 2011)
114 (the first step of nitrification), elevating NH_4^+ concentrations at the expense of NO_3^- . All of these
115 changes are expected to increase $\text{NH}_4^+:\text{DIN}$ ratios in marine environments. However, the
116 magnitude of NH_4^+ enrichment and its dominant drivers remain unquantified. Moreover, we lack
117 a general understanding as to the degree to which diatoms are negatively affected by NH_4^+
118 enrichment at the global scale. This represents an important knowledge gap as to how climate
119 change will affect the upper ocean nitrogen cycle and phytoplankton community composition,
120 with implications for carbon export and fisheries productivity. In this work, we use compilations
121 of phytoplankton relative abundance data and an ocean-biogeochemical model to quantify future
122 NH_4^+ enrichment and its effects on diatoms within the global ocean.

123 **2 Materials and Methods**

124 2.1 The biogeochemical model

125 The biogeochemical model is the Pelagic Interactions Scheme for Carbon and Ecosystem Studies
126 version 2 (PISCES-v2) (Aumont et al., 2015). This model is embedded within version 4.0 of the
127 Nucleus for European Modelling of the Ocean (NEMO-v4.0). We chose a 2° nominal horizontal
128 resolution with 31 vertical levels with thicknesses ranging from 10 meters in the upper 100
129 meters to 500 meters below 2000 meters. Due to the curvilinear grid, horizontal resolution
130 increases to 0.5° at the equator and to near 1° poleward of 50°N and 50°S .

131 We updated the standard PISCES-v2 for the purposes of this study. This model explicitly
132 resolves the pools of ammonium (NH_4^+), nitrite (NO_2^-), nitrate (NO_3^-), two kinds of

133 phytoplankton biomass (nanophytoplankton and diatoms), two kinds of zooplankton biomass
134 (micro- and meso-zooplankton), small and large pools of particulate organic matter, and
135 dissolved organic matter. Nitrogen is added to the ocean via biological nitrogen fixation, riverine
136 fluxes, and atmospheric deposition. Nitrogen is removed from the ocean via denitrification,
137 anaerobic ammonium oxidation (anammox) and burial. The internal cycling of nitrogen involves
138 assimilation by phytoplankton in particulate organic matter, grazing and excretion by
139 zooplankton, solubilization of particulates to dissolved organics, ammonification of dissolved
140 organic matter to NH_4^+ , followed by nitrification of NH_4^+ and NO_2^- via ammonia oxidation and
141 nitrite oxidation.

142 Of relevance to this study are the sources and sinks of NH_4^+ . Sources of NH_4^+ are
143 ammonification, zooplankton excretion and nitrogen fixation, while sinks are phytoplankton
144 assimilation, ammonia oxidation and anammox (Fig. S1). Each process is dependent on other
145 tracers and seawater properties (described in Aumont et al. (2015)). However, we briefly detail
146 the contribution to the NH_4^+ budget (mean \pm standard deviation) as well as primary dependencies
147 of the most important processes. Ammonification ($69 \pm 13\%$ of NH_4^+ sources) rates are highest
148 in productive oceanic regions with high concentrations of dissolved organic compounds.
149 Excretion of NH_4^+ by zooplankton ($30 \pm 13\%$ of sources) is modelled as a fraction of their
150 grazing rate, with this fraction ranging between 0.21 to 0.42 as phytoplankton become more
151 nutrient limited and are of poorer food quality. Phytoplankton assimilation of NH_4^+ ($62 \pm 27\%$ of
152 sinks) is modelled by multiplying a temperature- and light-dependent growth rate against
153 phytoplankton biomass, and subsequently applying limitations associated with nutrient
154 availability. Ammonia oxidation ($38 \pm 27\%$ of sinks) is modelled by multiplying a temperature-
155 dependent growth rate against the concentration of NH_4^+ and applying observationally-informed
156 limitation terms associated with NH_4^+ affinity, light intensity, and pH (Text S1). Phytoplankton
157 assimilation was a greater proportion of sinks in stratified, oligotrophic environments (Fig. S1).

158 2.2 Model experiments

159 To quantify the impact of anthropogenic activities on $\text{NH}_4^+:\text{DIN}$ ratios, we performed transient
160 simulations by forcing the biogeochemical model with monthly physical outputs produced by the
161 Institut Pierre-Simon Laplace Climate Model 5A (Dufresne et al., 2013). Simulations included a
162 preindustrial control where land-use, greenhouse gases and ozone remained at preindustrial

163 conditions, and a climate change run where these factors changed according to historical
164 observations from 1850 to 2005 and according to the high emissions Representative
165 Concentration Pathway 8.5 from 2006 to 2100 (RCP8.5) (Riahi et al., 2011). We chose a high
166 emissions scenario to emphasize the clearest degree of anthropogenic changes, and thus
167 maximize anthropogenic effects. However, we acknowledge that the RCP8.5 is considered an
168 extreme scenario under present development pathways (Riahi et al., 2017).

169 In addition, we performed parallel experiments that isolated the individual effects of our three
170 anthropogenic stressors: a changing circulation (“Phys”), warming on biological metabolism
171 (“Warm”), and acidification effects on ammonia oxidation (“OA”). The experiment with all
172 anthropogenic effects was termed “All”. These experiments involved altering the factor of
173 interest in line with the historical and RCP8.5 scenario while holding the other factors at their
174 preindustrial state.

175 The effect of climate change at the end of the 21st century (mean conditions 2081-2100) was
176 quantified by comparing with the preindustrial control simulation. This preindustrial control
177 simulation was run parallel to the climate change simulations (i.e., 1850-2100), but without
178 anthropogenic forcings. This allowed a direct comparison to be made between experiments at the
179 end of the 21st century and eliminated the effect of model drift. We calculated changes at each
180 grid cell by averaging over the euphotic zone, which was defined as those depths where total
181 phytoplankton biomass was greater than 0.1 mmol C m⁻³. In addition, we compared the
182 preindustrial simulation with observations to explore broad patterns in NH₄⁺ and NH₄⁺:DIN
183 ratios, averaged over the euphotic zone (Text S2; Fig. S2-S3).

184 Finally, we repeated the set of experiments described above (All, Phys, Warm and OA) but with
185 an alternative parameterization where diatoms were made to have the same growth limitation on
186 NH₄⁺ as other phytoplankton (Fig. S4). This experiment was called “model_{compete}”, while the
187 model with the default parameterization for nitrogen limitation was termed “model_{control}”.

188 2.3 Nutrient and rate data

189 Measured NH₄⁺ concentrations (N=692) were used for model-data assessment (Fig. S2-S3).
190 Nutrients were collated from published work (Buchwald et al., 2015; Mduyana et al., 2020;
191 Newell et al., 2013; Raes et al., 2020; A. E. Santoro et al., 2013; Alyson E. Santoro et al., 2021;

192 Shiozaki et al., 2016; Tolar et al., 2016; Xianhui S. Wan et al., 2021; Xianhui Sean Wan et al.,
193 2018), and oceanographic cruises AR16 (<https://www.bco-dmo.org/deployment/747056>), JC156,
194 and JC150. Coincident NO_2^- and NO_3^- were used to compute NH_4^+ to DIN ratios. If coincident
195 measurements of NO_2^- were not available, then NH_4^+ to DIN ratios were calculated with only
196 NO_3^- . If NO_3^- measurements were not made alongside NH_4^+ , then NO_3^- concentrations were
197 extracted from the World Ocean Atlas 2018 (Garcia et al., 2019) monthly climatology at the
198 closest grid cell. These data are available in Data Set S1.

199 Measured ammonia oxidation rates (N=696) were also used for model-data assessment and
200 showed broad agreement with the model (Fig. S5). Data were collated from published work
201 (Clark et al., 2021; Dore & Karl, 1996; Mdotyana et al., 2020; Newell et al., 2013; Raes et al.,
202 2020; Raimbault et al., 1999; A. E. Santoro et al., 2013; Alyson E. Santoro et al., 2021; Shiozaki
203 et al., 2016; Tolar et al., 2016; Xianhui S. Wan et al., 2021; Xianhui Sean Wan et al., 2018) and
204 are available in Data Set S2.

205 Measurements of NH_4^+ and NO_3^- concentrations alongside NH_4^+ - and NO_3^- -fueled primary
206 production ($\mu\text{mol m}^{-3} \text{ day}^{-1}$) were used to determine the relationship between NH_4^+ :DIN ratios
207 and the proportion of net primary production that is fueled by NH_4^+ (Fig. S6). While coincident
208 measurements of these properties are not common, we compiled data from nine studies
209 (Fernández et al., 2009; Joubert et al., 2011; Mdotyana et al., 2020; Metzler et al., 1997;
210 Philibert, 2015; Rees et al., 2006; Thomalla et al., 2011; Xianhui Sean Wan et al., 2018;
211 Yingling et al., 2021) providing 190 data points that together encompassed oligotrophic to
212 eutrophic conditions from the tropics to the Southern Ocean. Measurements from the Gulf of
213 Mexico (Yingling et al., 2021) were unique in that nutrient concentrations and uptake rates were
214 not measured at precisely the same depths or stations. Coincident values were determined by
215 calculating trends in depth via linear interpolation (Fig. S7). These data are available in Data Set
216 S3.

217 Ammonia oxidation rates data from experiments involving pH changes were acquired directly
218 from the papers presenting the results (Beman et al., 2011; Huesemann et al., 2002; Kitidis et al.,
219 2011) by extraction from the text (where values were given) and from figures using the
220 WebPlotDigitizer tool (<https://automeris.io/WebPlotDigitizer/>). Changes in ammonia oxidation
221 rates were normalized to a pH of 8 (Fig. S8). These data are available in Data Set S4.

2.4 Phytoplankton relative abundance data

222 *Tara* Oceans expeditions between 2009 and 2013 performed a worldwide sampling of plankton
 223 in the upper layers of the ocean (Pierella Karlusich et al., 2020). We mined the 18S rRNA gene
 224 (V9 region) metabarcoding data set (Ibarbalz et al., 2019; de Vargas et al., 2015) by retrieving
 225 the operational taxonomic units (OTUs) assigned to eukaryotic phytoplankton from samples
 226 obtained from 144 stations (<https://zenodo.org/record/3768510#.Xraby6gzY2w>). Barcodes with
 227 greater than 85 % identity to phytoplankton sequences in reference databases were selected. The
 228 total diatom barcode reads in each sample was normalized to the barcode read abundance of
 229 eukaryotic phytoplankton. We exclusively used the data sets corresponding to surface samples
 230 (5-9 m depth).
 231

232 In addition, we analyzed the metagenomic read abundances for the single-copy photosynthetic
 233 gene *psbO*, an approach that covers both cyanobacteria and eukaryotic phytoplankton and
 234 provides a more robust picture of phytoplankton cell abundances than rRNA gene methods
 235 (Pierella Karlusich et al., 2022). We retrieved the abundance tables from samples obtained from
 236 145 stations (<https://www.ebi.ac.uk/biostudies/studies/S-BSST761>).

2.5 Statistical analysis

237 We explored the environmental drivers of change in phytoplankton relative abundance data
 238 (provided by *Tara* Oceans) with generalized additive models (GAMs) using the *mgcv* package in
 239 R (Wood, 2006) according to the equation:
 240

$$Y = \alpha + s_1(x_1) + s_2(x_2) + \dots + s_n(x_n) + \varepsilon, \quad 1$$

241 Where Y is the predicted value of the response variable, α is the intercept, $s_n(x_n)$ is the n^{th} thin-
 242 plate spline of the n^{th} independent variable, and ε is the population error around the prediction.
 243 Independent variables were mixed-layer depth (m), phosphate (μM), silicate (μM), dissolved
 244 iron (μM), and the $\text{NH}_4^+:\text{DIN}$ ratio. Mixed layer depth, phosphate and silicate was measured *in*
 245 *situ* at the sample locations of *Tara* Oceans, while dissolved iron and $\text{NH}_4^+:\text{DIN}$ ratios were
 246 provided by the model. In addition, phosphate and silicate concentrations were available as
 247 interpolated products from the World Ocean Atlas (Garcia et al., 2019). An alternative estimate
 248 of $\text{NH}_4^+:\text{DIN}$ ratios was provided by the Darwin model (Follows et al., 2007). Predictor variables
 249 from models and World Ocean Atlas were extracted at the locations and months of sampling.

250 Mixed-layer depth, nutrients (phosphate, silicate and NH_4^+ :DIN) and the relative abundance of
251 phytoplankton taxa were \log_{10} -transformed prior to model building to ensure homogeneity of
252 variance.

253 Before model testing, we calculated the variance inflation factors (VIFs) of independent
254 variables to avoid multi-collinearity. All covariate VIFs were < 3 . GAMs were computed using a
255 low spline complexity ($k = 3$) that prevented overfitting. We fit GAMs using all predictors (full
256 model), then assessed the deviance explained by each predictor by fitting subsequent GAMs
257 with each predictor in isolation, and by removing the predictor in question from the full model.
258 The significance of a predictor was assessed by applying a smoothing penalty to only that
259 predictor in the full model. Diagnostic plots were assessed visually, and predictive capacity was
260 assessed via the percent of deviance explained by the model.

261 A two-sided Mann-Whitney U test was used to test for differences between the two distributions
262 of diatom relative abundance separated by NH_4^+ :DIN ratios $< 4\%$ and $> 4\%$ presented in Figure
263 2b. The 4% threshold was used because it split the dataset in half and aligned with the point at
264 which primary production transitioned from mostly new (NO_3^- -fueled) to regenerated (NH_4^+ -
265 fueled) (Fig. S6). This non-parametric test (performed with the *scipy* package in python) returned
266 highly significant two-sided p-values ($p < 0.0001$) where indicated by *** in Figure 2c

267 **3 Results and Discussion**

268 3.1 NH_4^+ enrichment and diatom relative abundance

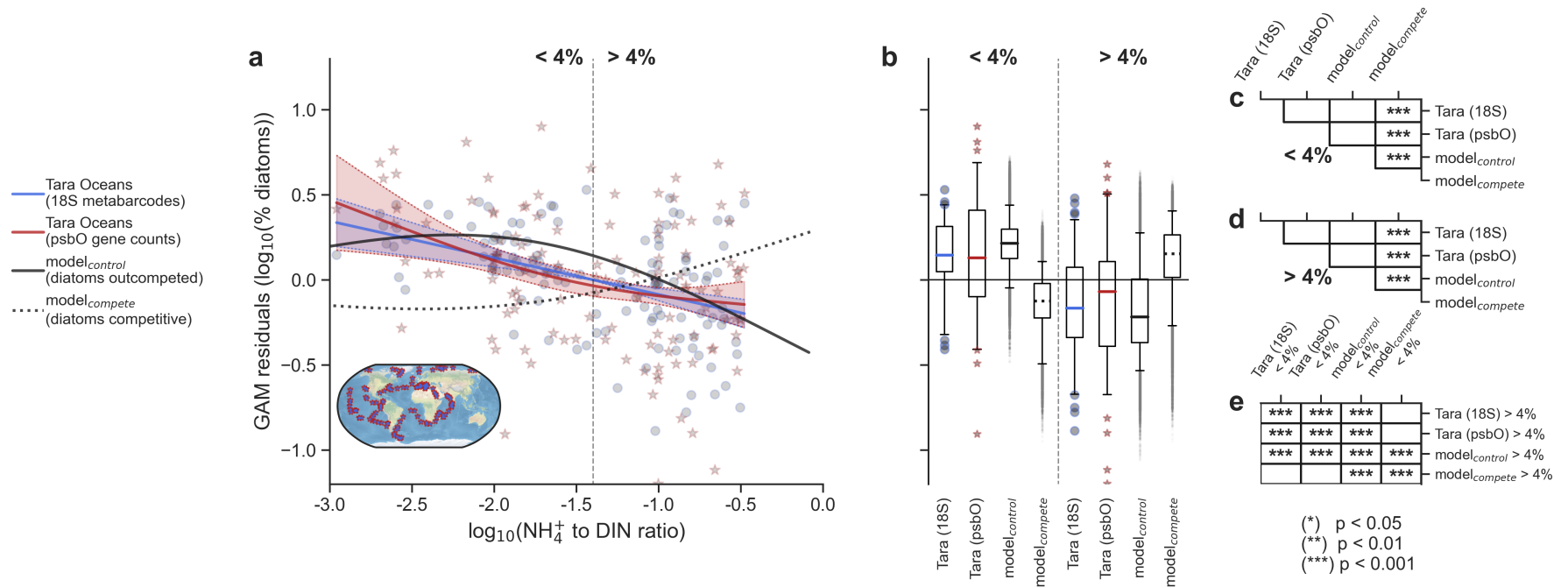
269 The competitive exclusion of diatoms by other phytoplankton in NH_4^+ enriched waters suggests
270 that declines in diatom relative abundance should be associated with increases in NH_4^+ :DIN.
271 While shown theoretically (Glibert et al., 2016; Litchman, 2007; Litchman et al., 2007) and in
272 restricted locations (Berg et al., 2003; Carter et al., 2005; Donald et al., 2013; Fawcett et al.,
273 2011; Klawonn et al., 2019; Van Oostende et al., 2017; Selph et al., 2021; Tungaraza et al.,
274 2003; Xianhui Sean Wan et al., 2018), this relationship is yet to be observed at the large scale.
275 The *Tara* Oceans global survey offers 144 stations encompassing equatorial to polar marine
276 environments (Ibarbalz et al., 2019). We used two proxies of diatom relative abundance from
277 this dataset: 18S rRNA gene metabarcodes for estimating relative abundance among eukaryotic
278 phytoplankton (de Vargas et al., 2015), and *psbO* gene counts for estimating relative abundance

279 among all phytoplankton (cyanobacteria and eukaryotes) (Pierella Karlusich et al., 2022). These
280 estimates were combined with $\text{NH}_4^+:\text{DIN}$ as predicted by a global ocean-biogeochemical model
281 (Aumont et al., 2015) at the same location and month of sampling, since NH_4^+ measurements are
282 scarce. This model effectively reproduced the sparse available datasets of NH_4^+ and $\text{NH}_4^+:\text{DIN}$,
283 and is aligned with current understanding of how NH_4^+ cycles in the ocean (Supplementary Text;
284 Fig. S1-S6). Model-derived $\text{NH}_4^+:\text{DIN}$ was used to predict diatom relative abundance in
285 Generalized Additive Models (GAMs), along with other bottom-up drivers of phytoplankton
286 community composition (see Methods).

287 Our analysis revealed that elevated $\text{NH}_4^+:\text{DIN}$ was consistently associated with declines in
288 diatom relative abundance (Fig. 2a). This negative relationship was evident and significant in
289 GAMs trained on both abundance proxies, as well as when using different combinations of
290 predictor variables: whether model-derived, *in situ* measurements, interpolated products (Garcia
291 et al., 2019), or when switching out $\text{NH}_4^+:\text{DIN}$ as predicted by our biogeochemical model with
292 that provided by another (Follows et al., 2007) (Table S1). Importantly, the relationship between
293 $\text{NH}_4^+:\text{DIN}$ and diatom relative abundance remained consistently negative and significant. This
294 was not the case for other predictors, which were prone to insignificance or sign changes
295 depending on the combination of predictors used (Fig. S9-S13). $\text{NH}_4^+:\text{DIN}$ also offered large
296 explanatory power for diatom abundance compared to the other predictor variables, explaining
297 between 18-30% of the deviance in the data (Table S1).

298 The association between diatoms and $\text{NH}_4^+:\text{DIN}$ was strong compared with the other major
299 phytoplankton taxa (Table S2). Only dinoflagellates (18S metabarcoding), *Prochlorococcus* and
300 chlorophytes (*psbO*) showed similarly strong associations (Fig. S14-S15). These associations are
301 also expected. *Prochlorococcus* was positively related to $\text{NH}_4^+:\text{DIN}$, reflecting their superior
302 affinity for NH_4^+ and dominance in oligotrophic gyres (Herrero et al., 2001; Litchman, 2007;
303 Litchman et al., 2007; Matsumoto et al., 2016; Rii et al., 2016). Chlorophytes were negatively
304 related to $\text{NH}_4^+:\text{DIN}$ and positively related to phosphate, reflecting their prominence in nutrient-
305 rich waters (Vannier et al., 2016). The positive relationship between dinoflagellates and
306 $\text{NH}_4^+:\text{DIN}$ within eukaryotic phytoplankton likely reflects the inclusion of non-photosynthetic
307 dinoflagellate lineages with the 18S metabarcoding method (Pierella Karlusich et al., 2022) and
308 the proliferation of these types within systems enriched in reduced nitrogen (Glibert et al., 2016).

309 We performed the same GAM analysis on diatom relative abundances predicted by our
310 biogeochemical model (model_{control}; black line in Fig. 2a). This model imbues its diatoms with a
311 known competitive disadvantage for NH_4^+ (Fig. 1a; Fig. S4). If competition for NH_4^+ is an
312 important control on diatom relative abundance in the model, we should therefore see a strong
313 negative relationship between the $\text{NH}_4^+:\text{DIN}$ ratio and diatom relative abundance. We stress here
314 that if diatoms had an equal affinity for NH_4^+ as other phytoplankton, then they would not be
315 outcompeted (as shown later). As expected, diatom relative abundance was negatively related to
316 $\text{NH}_4^+:\text{DIN}$ (deviance explained = 70%; p-value < 0.001). Interestingly, the relationship was also
317 strongly non-linear and similar to that seen in the *Tara* Oceans data, with rapid losses of diatoms
318 as $\text{NH}_4^+:\text{DIN}$ became greater than 4%. This threshold, where NH_4^+ becomes 4% of total nitrogen
319 stocks, aligns with the point at which primary production becomes dominated by regenerated
320 production (Fig. S6). This result not only showcases the intense recycling of NH_4^+ in the marine
321 environment and competition for this coveted nutrient, but also showcases how diatoms are
322 outcompeted as more primary production becomes regenerated. On the other hand, this also
323 showcases how diatom are major contributors to new primary production in the ocean (Fawcett
324 et al., 2011). Importantly, on either side of this 4% threshold, the GAM predictions built from
325 both the biogeochemical model and *Tara* Oceans data could not be statistically differentiated
326 (Fig. 2b,c,d; Mann-Whitney U pair-wise tests). Both modelled and *Tara* Oceans data predicted
327 similar values of diatom relative abundance within communities where $\text{NH}_4^+:\text{DIN}$ was less than
328 4%, as well as in communities where $\text{NH}_4^+:\text{DIN}$ was greater than 4% (Fig. 2b,e). Overall, the
329 modelled and observed changes in diatom relative abundance associated with $\text{NH}_4^+:\text{DIN}$ appear
330 statistically indistinguishable. Since our biogeochemical model explicitly accounts for
331 competitive exclusion of diatoms as $\text{NH}_4^+:\text{DIN}$ increases, this similarity may mean that the
332 negative relationship apparent in both may originate from the same mechanism, specifically
333 being a competitive disadvantage for NH_4^+ .



334

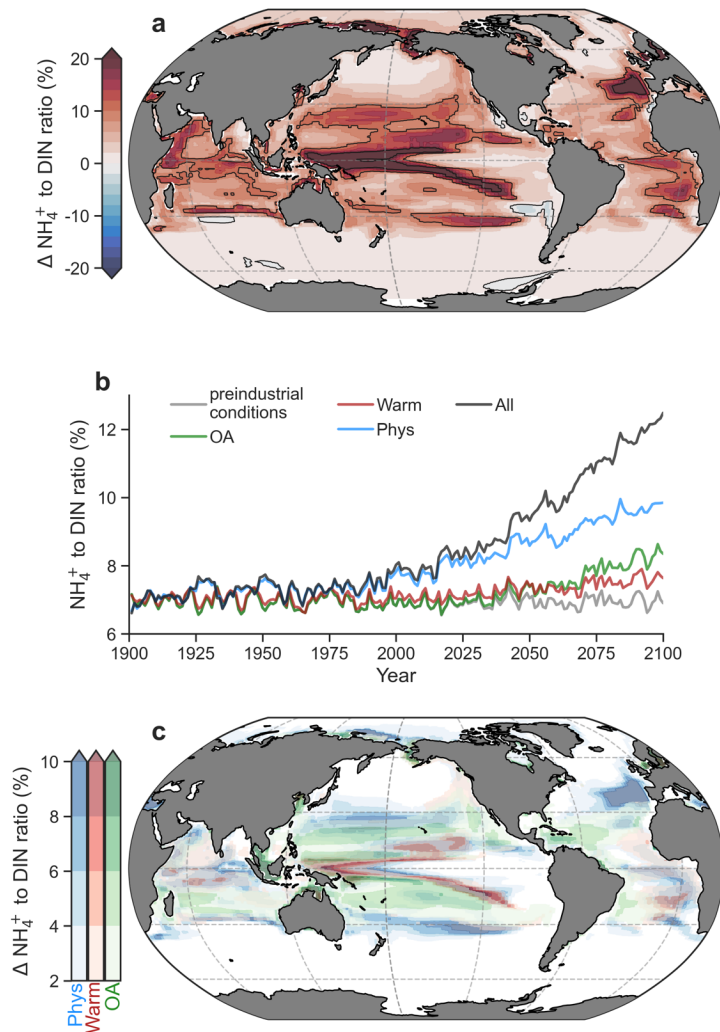
335 **Fig. 2. Effects of NH_4^+ enrichment on primary production and diatom relative abundance.** (a), Partial dependence plot from the
 336 generalized additive model (GAM) showing the relationship between the NH_4^+ to DIN ratio and the percent relative abundance of
 337 diatoms. Blue round markers and blue line fit are percent among eukaryotic phytoplankton (18S rRNA metabarcodes). Red star
 338 markers and red line fit are percent among all phytoplankton (*psbO* gene counts). Solid and dashed black lines are output from the
 339 ocean-biogeochemical model with and without competitive exclusion of diatoms for NH_4^+ . The vertical dotted line delineates when
 340 NH_4^+ is 4% of DIN. The inset map shows the locations of *Tara* Oceans samples. (b), Boxplots of the raw partial residuals from panel
 341 (a) but separated either side of the 4% NH_4^+ to DIN threshold for percent among eukaryotic phytoplankton (blue), all phytoplankton
 342 (red), the ocean-biogeochemical model (solid black), and model without competitive exclusion of diatoms for NH_4^+ (dashed black).
 343 Whiskers correspond to the 5th and 95th percentiles. Tables on the right denote significant pair-wise differences (Mann-Whitney U)
 344 amongst datasets when $\text{NH}_4^+:\text{DIN}$ is less than 4% (c), when it is more than 4% (d) and when comparing < 4% with > 4% datasets (e).

3.2 Future enrichment of NH_4^+ in the ocean

345
346 Given the importance of NH_4^+ enrichment for influencing primary production and phytoplankton
347 community composition, we explored the potential impact of anthropogenic climate change on
348 $\text{NH}_4^+:\text{DIN}$ across the global ocean. Using a high emissions climate change scenario from 1851 to
349 2100 (Representative Concentration Pathway 8.5 (Riahi et al., 2011)), we simulated physical
350 changes (circulation change + sea-ice loss), the stimulation of metabolism by warming, and a
351 data-constrained slowdown of ammonia oxidation by ocean acidification (Fig. S16) in our ocean-
352 biogeochemical model. By the end of the 21st century (2081-2100), these factors increased
353 $\text{NH}_4^+:\text{DIN}$ in over 98% of the upper ocean euphotic layer (Fig. 3a). On average, the fraction of
354 DIN present as NH_4^+ increased by $6 \pm 6\%$, with enrichment exceeding 20% in regions with
355 pronounced DIN gradients, such as oceanographic fronts. The enrichment of NH_4^+ caused an
356 expansion of regenerated production across the ocean, such that NH_4^+ overtook NO_3^- as the main
357 nitrogen substrate for phytoplankton growth in an additional 13% of the ocean. The greatest
358 change occurred within the 21st century (Fig. 3b), indicating a direct relationship between the
359 severity of climate change and the magnitude of NH_4^+ enrichment.

360 Physical changes, a warming-induced stimulation of microbial metabolism and ocean
361 acidification all played a role in increasing $\text{NH}_4^+:\text{DIN}$. Among these factors, physical changes
362 had the largest contribution, accounting for 55% of future trends (Fig. 3b), followed by ocean
363 acidification (25%) and stimulated metabolism (13%). Physical changes decreased DIN to cause
364 increases in $\text{NH}_4^+:\text{DIN}$ in many regions (Fig 3c; Fig. S16) and occurred either through reduced
365 physical supply (e.g., North Atlantic (Whitt & Jansen, 2020)) or increased demand and export of
366 organic nitrogen in regions experiencing an increase in primary production due to losses in sea
367 ice and increases in light (e.g., Arctic (Comeau et al., 2011)). Ocean acidification increased
368 $\text{NH}_4^+:\text{DIN}$ everywhere, but had the greatest effect in oligotrophic settings where DIN
369 concentrations are lower, and minimal effects in eutrophic regions (Fig 3c; Fig. S16). We do
370 note, however, that there is much uncertainty in the relationship between pH and ammonia
371 oxidation rates (Bayer et al., 2016; Kitidis et al., 2011). We performed an idealized experiment
372 exploring a much weaker relationship between pH and ammonia oxidation that reduced the
373 contribution of acidification to NH_4^+ enrichment by 10% or more and increased the contribution
374 of the other stressors (Fig. S17). However, as pH decline was most strongly influential to

375 NH_4^+ :DIN ratios in the subtropical gyres, the alternative parameterization did little to change
 376 NH_4^+ :DIN ratios in eutrophic regions where diatoms form an important component on the
 377 community. Warming stimulated the nutrient demand of phytoplankton, which reduced DIN, a
 378 mechanism consistent with the effects of temperature on marine microbial recycling (Cherabier
 379 & Ferrière, 2022). While its global contribution was small at 13% (Fig. 3b), warming had
 380 important effects at the boundaries of NO_3^- -rich regions by contracting their areal extent, turning
 381 NO_3^- -rich waters to NO_3^- -poor waters (Fig. 3c; Fig. S16). Altogether, the individual contributions
 382 of physical change, acidification and stimulated metabolism diagnosed via our sensitivity
 383 experiments explained 93% of the full change in NH_4^+ :DIN, indicating that a linear combination
 384 of the three drivers accounted for near the full response.



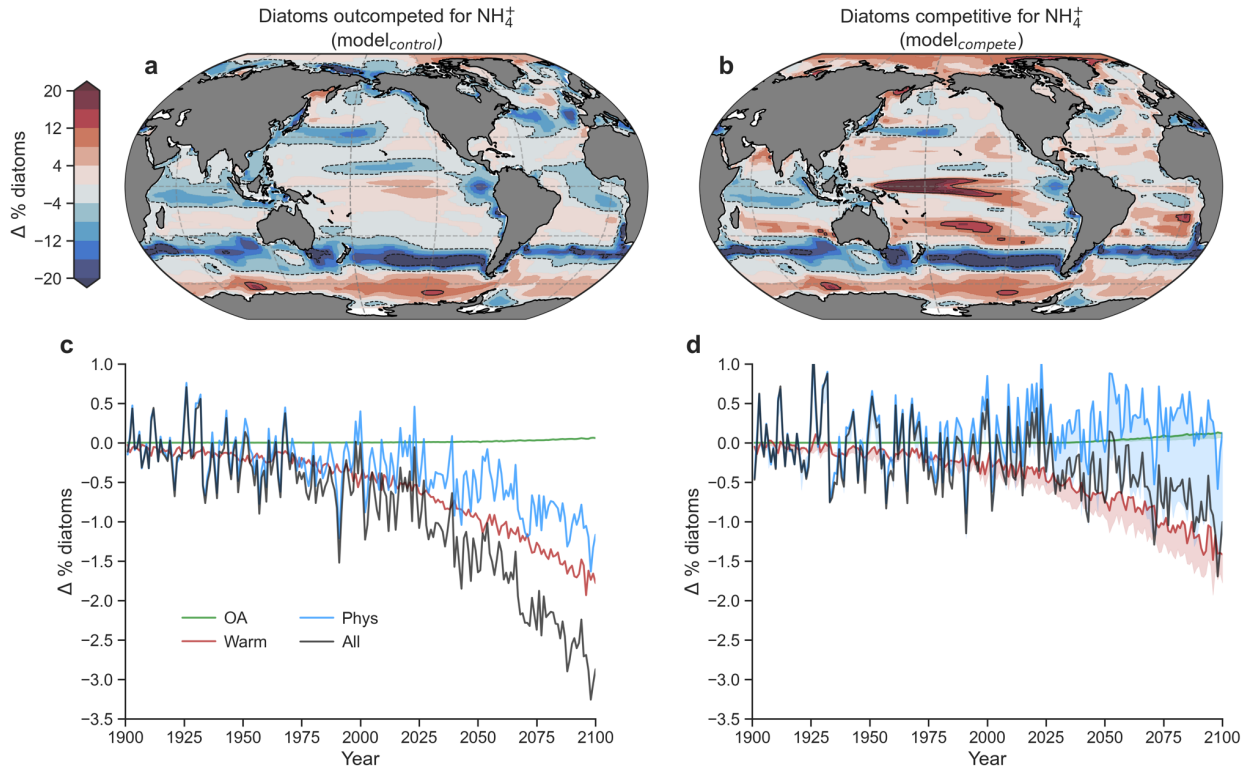
385

386 **Fig. 3. Anthropogenic impacts on the NH_4^+ to DIN ratio.** (a), The difference in the NH_4^+ to
387 DIN ratio averaged over the euphotic zone at the end of the 21st century (2081-2100) with all
388 anthropogenic impacts. (b), Global mean trends in euphotic zone NH_4^+ to DIN ratio in the
389 different experiments: preindustrial control (grey), ocean acidification (OA; green), warming on
390 metabolic rates (Warm; red), physical changes (Phys; blue) and all effects (All; black) according
391 to the RCP8.5 climate change scenario. (c), Increases in the NH_4^+ to DIN ratio due to physical
392 changes (blue), effect of warming on metabolic rates (red) and ocean acidification on ammonia
393 oxidation (green) from a multiple stressor perspective.

394

395 3.3 Impacts on future diatom abundance

396 Our climate change simulations predict a future decline in the abundance of diatoms and their
397 representation within phytoplankton communities, particularly in the subantarctic, tropical, North
398 Atlantic, North Pacific and Arctic Oceans where declines sometimes exceeded 20% (Fig. 4a; Fig.
399 S18). Diatoms are currently major contributors to net primary production in these regions
400 (Armbrust, 2009; Tréguer et al., 2018; Uitz et al., 2010). The decline in diatom relative
401 abundance was driven by a combination of stimulated microbial metabolism (60%) and physical
402 changes (40%), while ocean acidification had negligible effects (Figure 4c) because of its limited
403 effect on $\text{NH}_4^+:\text{DIN}$ outside of the oligotrophic gyres where diatoms are already a small
404 proportion of communities (Fig. S17). However, we recognize that other influential bottom-up
405 and top-down stressors, such as growth limitation by other nutrients (Taucher et al., 2022), shifts
406 in the light environment, and/or grazing pressure (Brun et al., 2015; Margalef, 1978; Taucher et
407 al., 2022) are also influential to structuring phytoplankton communities. Furthermore, we
408 acknowledge that the negative relationship that we observe between $\text{NH}_4^+:\text{DIN}$ and diatom
409 relative abundance in both the *Tara* Oceans datasets and the model (Figure 2a) may be
410 influenced by these or other covarying factors. This includes increases or decreases in the total
411 availability of DIN, namely being NO_3^- . If other factors are covarying with $\text{NH}_4^+:\text{DIN}$ but are
412 more influential to diatom relative abundance, this may lead to the erroneous attribution of a
413 causative relationship between diatom relative abundance and $\text{NH}_4^+:\text{DIN}$ ratios (i.e., a false
414 positive).



415

416 **Fig. 4. Impact of NH_4^+ enrichment within DIN on diatom relative abundance.** (a), Mean
 417 change (Δ) in the relative abundance of diatoms (%) by the end of the 21st century (2081-2100)
 418 as predicted by the control run of the ocean-biogeochemical model ($\text{model}_{\text{control}}$) under the
 419 RCP8.5 scenario and averaged over the euphotic zone. (b), Same as in (a), but for the model
 420 with equal affinities of diatoms and other phytoplankton for NH_4^+ ($\text{model}_{\text{compete}}$). (c), Global
 421 mean change in diatom relative abundance due to physical (circulation + light) changes (blue),
 422 warming effects on metabolic rates (red), ocean acidification effect on ammonia oxidation
 423 (green) and all stressors (black) for $\text{model}_{\text{control}}$. (d), The same as in (c), but for $\text{model}_{\text{compete}}$.
 424 Shading shows the change between (c) and (d).

425

426 To isolate the impact of competition for NH_4^+ specifically, and thus target the causative
 427 relationship between $\text{NH}_4^+:\text{DIN}$ and diatom relative abundance, we performed idealized
 428 experiments that equalized diatom growth limitation on NH_4^+ with that of other phytoplankton
 429 ($\text{model}_{\text{compete}}$; equivalent to making the dashed lines in Figure 1a equivalent; Fig. S4). All other
 430 traits remained unchanged, including the different affinities of diatoms and other phytoplankton
 431 for NO_3^- . This experiment meant that when DIN was low, diatoms were equally competitive for

432 NH_4^+ , but still suffered their unique limitations associated with light, silicate, phosphate, nitrate
433 (Fig. 1a) and iron availability, as well as grazing pressure.

434 Making diatoms equally competitive for NH_4^+ mitigated the losses of diatom representation
435 within future phytoplankton communities by 70%. While phytoplankton biomass, including
436 diatoms, largely declined everywhere outside of the polar regions (Fig. S18), the losses in diatom
437 relative abundance were reduced from a global mean of 3.2% to 0.9% by 2081-2100 (Fig. 4c).
438 Physical changes no longer exerted a global negative effect on their total nor relative abundance,
439 while the negative effect of elevated microbial metabolism on relative abundance was
440 ameliorated by 25% (Fig. 4d; Fig. S18-19). Diatoms even showed increased total and/or relative
441 abundance in regions where previously there were losses, including the Arctic, the tropical
442 Pacific, the Arabian Sea, the North Atlantic, and the southern subtropics. Outside of the Southern
443 Ocean and the eastern boundary upwelling systems, physical changes that tended to reduce DIN
444 concentrations now favored diatoms, while elevated metabolism now had positive, rather than
445 negative, effects in the tropical Pacific.

446 These experiments provide valuable insights into the factors controlling diatom niches. Regions
447 where $\text{model}_{\text{control}}$ and $\text{model}_{\text{compete}}$ show similar changes are regions where other factors besides
448 $\text{NH}_4^+:\text{DIN}$ determine diatom competitiveness. In the Southern Ocean, iron, light and silicic acid
449 are the major controls on diatom productivity and phytoplankton community composition (P.
450 Boyd et al., 1999; P. W. Boyd et al., 2000; Krumhardt et al., 2022; Llort et al., 2019), and this is
451 apparent in the matching outcomes of $\text{model}_{\text{control}}$ and $\text{model}_{\text{compete}}$. However, where $\text{model}_{\text{control}}$
452 and $\text{model}_{\text{compete}}$ predicted contrasting outcomes, the form of nitrogen, specifically $\text{NH}_4^+:\text{DIN}$
453 and thus the intense competition for NH_4^+ , exerted a dominant control.

454 The importance of phytoplankton's competitive ability for NH_4^+ is exemplified by the fact that
455 the negative relationship between $\text{NH}_4^+:\text{DIN}$ and diatom relative abundance was reversed in
456 $\text{model}_{\text{compete}}$ (black dotted line in Fig. 2a). Now positive rather than negative, this relationship
457 differed statistically from those predicted from *Tara* Oceans data (Figure 2b-e). This strongly
458 suggests that competition for NH_4^+ independently controls diatom relative abundance. We stress
459 that in this experiment both diatoms and other phytoplankton maintained the same affinity for
460 NO_3^- . While we acknowledge that decreases in NO_3^- were a major cause of NH_4^+ enrichment in
461 our experiments, we emphasize that the mechanism by which diatoms decline in the community

462 is due to their poor competitive ability for growth on NH_4^+ , not because of increases or decreases
463 in total NO_3^- concentration. Changes in NO_3^- certainly affect diatom growth, but only do so
464 indirectly by shifting the regime away from or towards intense competition for NH_4^+ . Given the
465 statistical similarity between the *in situ* (*Tara Oceans*) and *in silico* ($\text{model}_{\text{control}}$) relationships,
466 this implicates $\text{NH}_4^+:\text{DIN}$ as a key underlying driver of diatom relative abundance in the world
467 ocean.

468 **4 Conclusions**

469 Our results show that the form of bioavailable nitrogen exerts a strong influence on the
470 competitive niche of diatoms, and that this niche is therefore tied to the upper ocean nitrogen
471 cycle. Our modelling suggests an enrichment of NH_4^+ in over 98% of ocean euphotic zones by
472 the end of the 21st century under a high emissions scenario (Riahi et al., 2011). In those places
473 where nitrogen availability limits growth, diatoms suffer displacement by phytoplankton taxa
474 with a greater affinity for NH_4^+ . The warming and physical changes that drive NH_4^+ enrichment
475 and diatom displacement are expected (Bindoff et al., 2019) and the link between NH_4^+
476 enrichment and diatom displacement is demonstrated herein at the global scale. However, we
477 acknowledge that the link between environmental change and NH_4^+ enrichment rests on
478 processes that are still not fully understood. For instance, an observed increase in summertime
479 mixed layer depths may counter the effect of a strengthening pycnocline (Sallée et al., 2021) to
480 increase NO_3^- injection into euphotic zones. Another key contributor to this uncertainty is the
481 microbial loop, driven by heterotrophic bacteria, which resupplies NH_4^+ through mineralization
482 of organic matter (Fig. 1b). The microbial loop is not yet incorporated in detail within earth
483 system models but its response to warming can either elevate or depress regenerated production
484 depending on assumptions made about the bacterial physiology (Cherabier & Ferrière, 2022).
485 The future balance of reduced (NH_4^+ and organic forms) to oxidized nitrogen and its impact on
486 the state of marine ecosystems hinges on a suite of unexplored feedbacks between the marine
487 microbial loop and environmental change.

488 Overall, the open ocean habitat appears to be becoming more challenging for diatoms. Iron stress
489 is growing in the Southern Ocean (Ryan-Keogh et al., 2023), silicic acid limitation is prospect
490 across the ocean in response to ocean acidification (Taucher et al., 2022), and growing nitrogen
491 limitation may make diatoms less adaptable as temperatures rise (Aranguren-Gassis et al., 2019).

492 Furthermore, diatoms may be even more susceptible to increases in NH_4^+ :DIN in temperate
493 waters, as cooler conditions appear to amplify their growth dependence on NO_3^- (Glibert et al.,
494 2016; Parker & Armbrust, 2005). In addition to these stressors, the climate-driven expansion of
495 NH_4^+ -enriched oligotrophic gyres, as well as the potential for a NO_3^- -limited Arctic, will further
496 disadvantage diatoms. Notwithstanding the potential for evolution, these and other rapid changes
497 may reduce diatom diversity (Lampe et al., 2018; Sugie et al., 2020), making diatoms susceptible
498 to extirpation (Cael et al., 2021). If this is realized, ocean ecosystems may shift towards longer,
499 less productive food-chains underpinned by smaller, slower-growing phytoplankton (Sommer et
500 al., 2002), with severe implications for the health of important fisheries and carbon storage.
501 Further work is urgently needed to understand how this key marine phytoplankton group might
502 respond to these growing challenges in an integrated manner.

503

504 **Acknowledgments**

505 Simulations and development were undertaken on Barkla, part of the High-Performance
506 Computing facilities at the University of Liverpool. The authors wish to acknowledge use of the
507 Ferret program (<http://ferret.pmel.noaa.gov/Ferret/>), climate data operators
508 (<https://code.mpimet.mpg.de/projects/cdo/>), NetCDF Operators (<http://nco.sourceforge.net/>) and
509 Python (www.python.org) for the analysis and graphics in this paper. Thanks to Xianhui Wan,
510 Carolyn Buchwald and Alyson Santoro who shared data, and ongoing discussions with Elena
511 Litchman. PJB, RET and AT were supported by the ARISE project (NE/P006035/1), part of the
512 Changing Arctic Ocean programme, jointly funded by the UKRI Natural Environmental
513 Research Council (NERC) and the German Federal Ministry of Education and Research
514 (BMBF). JPK was supported by the Moore-Simons Project on the Origin of the Eukaryotic Cell,
515 Simons Foundation (735929LPI). EMSW and AT acknowledge support from the UKRI NERC
516 grant NE/N009525/1, the Mid Atlantic Ridge project (FRidge). EMSW was also supported by
517 the UKRI NERC grant NE/N001079/1 (Zinc, Iron and Phosphorus in the Atlantic). CB
518 acknowledges support from FEM (Fonds Francais pour l'Environnement Mondial), the French
519 Government 'Investissements d'Avenir' programs OCEANOMICS (ANR-11-BTBR-0008),
520 FRANCE GENOMIQUE (ANR-10-INBS-09-08), MEMO LIFE (ANR-10-LABX-54), and PSL
521 Research University (ANR-11-IDEX-0001-02), the European Research Council (ERC) under the

522 European Union's Horizon 2020 research and innovation program (Diatomic; grant agreement
523 No. 835067), and project AtlantECO.

524

525 **Open Research**

526 All data and materials used in the analysis are freely available. Nutrient data, nitrification rates,
527 coincident nutrient concentrations with regenerated/new primary production rates, and ammonia
528 oxidation rates relative to pH variations are provided in Supplementary Data 1-4. The biological
529 data from the *Tara* Oceans sampling program are available at

530 <https://zenodo.org/record/3768510#.Xraby6gzY2w> and [https://ftp.ebi.ac.uk/biostudies/nfs/S-](https://ftp.ebi.ac.uk/biostudies/nfs/S-BSST/761/S-BSST761/)

531 [BSST/761/S-BSST761/](https://ftp.ebi.ac.uk/biostudies/nfs/S-BSST/761/S-BSST761/). The model output and scripts to reproduce the analysis are available at

532 <https://doi.org/10.5281/zenodo.7630283>. Developments to the PISCESv2 ocean-biogeochemical
533 model code are freely available for download at

534 https://github.com/pearseb/ORCA2_OFF_PISCESiso-N.

535

536 **References**

- 537 Aranguren-Gassis, M., Kremer, C. T., Klausmeier, C. A., & Litchman, E. (2019). Nitrogen limitation inhibits marine
538 diatom adaptation to high temperatures. *Ecology Letters*, 22(11), 1860–1869.
539 <https://doi.org/10.1111/ele.13378>
- 540 Armbrust, E. V. (2009). The life of diatoms in the world's oceans. *Nature*, 459(7244), 185–192.
541 <https://doi.org/10.1038/nature08057>
- 542 Arsenieff, L., Le Gall, F., Rigaut-Jalabert, F., Mahé, F., Sarno, D., Gouhier, L., et al. (2020). Diversity and dynamics
543 of relevant nanoplanktonic diatoms in the Western English Channel. *The ISME Journal*, 14(8), 1966–1981.
544 <https://doi.org/10.1038/s41396-020-0659-6>
- 545 Aumont, O., Ethé, C., Tagliabue, A., Bopp, L., & Gehlen, M. (2015). PISCES-v2: an ocean biogeochemical model
546 for carbon and ecosystem studies. *Geoscientific Model Development*, 8(8), 2465–2513.
547 <https://doi.org/10.5194/gmd-8-2465-2015>
- 548 Babbin, A. R., Buchwald, C., Morel, F. M. M., Wankel, S. D., & Ward, B. B. (2020). Nitrite oxidation exceeds
549 reduction and fixed nitrogen loss in anoxic Pacific waters. *Marine Chemistry*, 224(April), 103814.
550 <https://doi.org/10.1016/j.marchem.2020.103814>
- 551 Bayer, B., Vojvoda, J., Offre, P., Alves, R. J. E., Elisabeth, N. H., Garcia, J. AL, et al. (2016). Physiological and
552 genomic characterization of two novel marine thaumarchaeal strains indicates niche differentiation. *The ISME*
553 *Journal*, 10(5), 1051–1063. <https://doi.org/10.1038/ismej.2015.200>
- 554 Bayer, B., McBeain, K., Carlson, C. A., & Santoro, A. E. (2022). Carbon content, carbon fixation yield and
555 dissolved organic carbon release from diverse marine nitrifiers. *Limnology and Oceanography*.
556 <https://doi.org/10.1002/lno.12252>
- 557 Beman, J. M., Chow, C. E., King, A. L., Feng, Y., Fuhrman, J. A., Andersson, A., et al. (2011). Global declines in
558 oceanic nitrification rates as a consequence of ocean acidification. *Proceedings of the National Academy of*
559 *Sciences of the United States of America*, 108(1), 208–213. <https://doi.org/10.1073/pnas.1011053108>
- 560 Bender, M. L., & Jönsson, B. (2016). Is seasonal net community production in the South Pacific Subtropical Gyre
561 anomalously low? *Geophysical Research Letters*, 43(18), 9757–9763. <https://doi.org/10.1002/2016GL070220>

- 562 Berg, G., Balode, M., Purina, I., Bekere, S., Béchemin, C., & Maestrini, S. (2003). Plankton community
563 composition in relation to availability and uptake of oxidized and reduced nitrogen. *Aquatic Microbial*
564 *Ecology*, 30(3), 263–274. <https://doi.org/10.3354/ame030263>
- 565 Bindoff, N. L., Cheung, W. W. L., Kairo, J. G., Aristegui, J., Guinder, V. A., Hallberg, R., et al. (2019). Changing
566 Ocean, Marine Ecosystems, and Dependent Communities. In H.-O. Portner, C. D. Roberts, V. Masson-
567 Delmotte, P. Zhai, E. Tignor, E. Poloczanska, et al. (Eds.), *IPCC Special Report on the Ocean and Cryosphere*
568 *in a Changing Climate* (pp. 447–588). <https://doi.org/https://www.ipcc.ch/report/srocc/>
- 569 Bopp, L., Aumont, O., Cadule, P., Alvain, S., & Gehlen, M. (2005). Response of diatoms distribution to global
570 warming and potential implications: A global model study. *Geophysical Research Letters*, 32(19), n/a-n/a.
571 <https://doi.org/10.1029/2005GL023653>
- 572 Boyd, P., LaRoche, J., Gall, M., Frew, R., & McKay, R. M. L. (1999). Role of iron, light, and silicate in controlling
573 algal biomass in subantarctic waters SE of New Zealand. *Journal of Geophysical Research: Oceans*, 104(C6),
574 13395–13408. <https://doi.org/10.1029/1999JC900009>
- 575 Boyd, P. W., Watson, A. J., Law, C. S., Abraham, E. R., Trull, T., Murdoch, R., et al. (2000). A mesoscale
576 phytoplankton bloom in the polar Southern Ocean stimulated by iron fertilization. *Nature*, 407(6805), 695–
577 702. <https://doi.org/10.1038/35037500>
- 578 Bristow, L. A., Dalsgaard, T., Tiano, L., Mills, D. B., Bertagnolli, A. D., Wright, J. J., et al. (2016). Ammonium and
579 nitrite oxidation at nanomolar oxygen concentrations in oxygen minimum zone waters. *Proceedings of the*
580 *National Academy of Sciences*, 113(38), 10601–10606. <https://doi.org/10.1073/pnas.1600359113>
- 581 Brun, P., Vogt, M., Payne, M. R., Gruber, N., O'Brien, C. J., Buitenhuis, E. T., et al. (2015). Ecological niches of
582 open ocean phytoplankton taxa. *Limnology and Oceanography*, 60(3), 1020–1038.
583 <https://doi.org/10.1002/lno.10074>
- 584 Buchanan, P. J., Aumont, O., Bopp, L., Mahaffey, C., & Tagliabue, A. (2021). Impact of intensifying nitrogen
585 limitation on ocean net primary production is fingerprinted by nitrogen isotopes. *Nature Communications*,
586 12(1), 6214. <https://doi.org/10.1038/s41467-021-26552-w>
- 587 Buchwald, C., Santoro, A. E., Stanley, R. H. R., & Casciotti, K. L. (2015). Nitrogen cycling in the secondary nitrite
588 maximum of the eastern tropical North Pacific off Costa Rica. *Global Biogeochemical Cycles*, 29(12), 2061–
589 2081. <https://doi.org/10.1002/2015GB005187>
- 590 Cael, B. B., Dutkiewicz, S., & Henson, S. (2021). Abrupt shifts in 21st-century plankton communities. *Science*
591 *Advances*, 7(44). <https://doi.org/10.1126/sciadv.abf8593>
- 592 Carter, C. M., Ross, A. H., Schiel, D. R., Howard-Williams, C., & Hayden, B. (2005). In situ microcosm
593 experiments on the influence of nitrate and light on phytoplankton community composition. *Journal of*
594 *Experimental Marine Biology and Ecology*, 326(1), 1–13. <https://doi.org/10.1016/j.jembe.2005.05.006>
- 595 Cherabier, P., & Ferrière, R. (2022). Eco-evolutionary responses of the microbial loop to surface ocean warming and
596 consequences for primary production. *ISME Journal*, 16(4), 1130–1139. [https://doi.org/10.1038/s41396-021-](https://doi.org/10.1038/s41396-021-01166-8)
597 01166-8
- 598 Clark, D. R., Rees, A. P., Ferrera, C., Al-moosawi, L., Somerfield, P. J., Harris, C., et al. (2021). Nitrification in the
599 oligotrophic Atlantic Ocean. *Biogeosciences Discussions*, (August), 1–29. [https://doi.org/10.5194/bg-2021-](https://doi.org/10.5194/bg-2021-184)
600 184
- 601 Comeau, A. M., Li, W. K. W., Tremblay, J.-É., Carmack, E. C., & Lovejoy, C. (2011). Arctic Ocean Microbial
602 Community Structure before and after the 2007 Record Sea Ice Minimum. *PLoS ONE*, 6(11), e27492.
603 <https://doi.org/10.1371/journal.pone.0027492>
- 604 Cushing, D. H. (1989). A difference in structure between ecosystems in strongly stratified waters and in those that
605 are only weakly stratified. *Journal of Plankton Research*, 11(1), 1–13. <https://doi.org/10.1093/plankt/11.1.1>
- 606 Donald, D. B., Bogard, M. J., Finlay, K., Bunting, L., & Leavitt, P. R. (2013). Phytoplankton-Specific Response to
607 Enrichment of Phosphorus-Rich Surface Waters with Ammonium, Nitrate, and Urea. *PLoS ONE*, 8(1),
608 e53277. <https://doi.org/10.1371/journal.pone.0053277>
- 609 Dore, J. E., & Karl, D. M. (1996). Nitrification in the euphotic zone as a source for nitrite, nitrate, and nitrous oxide
610 at Station ALOHA. *Limnology and Oceanography*, 41(8), 1619–1628.
611 <https://doi.org/10.4319/lo.1996.41.8.1619>
- 612 Dufresne, J. L., Foujols, M. A., Denvil, S., Caubel, A., Marti, O., Aumont, O., et al. (2013). *Climate change*
613 *projections using the IPSL-CM5 Earth System Model: From CMIP3 to CMIP5. Climate Dynamics* (Vol. 40).
614 <https://doi.org/10.1007/s00382-012-1636-1>
- 615 Dugdale, R. C., & Goering, J. J. (1967). Uptake of New and Regenerated Forms of Nitrogen in Primary
616 Productivity. *Limnology and Oceanography*, 12(2), 196–206. <https://doi.org/10.4319/lo.1967.12.2.0196>
- 617 Eppley, R. W. (1972). Temperature and phytoplankton growth in the sea. *Fishery Bulletin*, 70(4), 1063–1085.

- 618 Eppley, R. W., & Peterson, B. J. (1979). Particulate organic matter flux and planktonic new production in the deep
619 ocean. *Nature*, 282(5740), 677–680. <https://doi.org/10.1038/282677a0>
- 620 Fawcett, S. E., Lomas, M. W., Casey, J. R., Ward, B. B., & Sigman, D. M. (2011). Assimilation of upwelled nitrate
621 by small eukaryotes in the Sargasso Sea. *Nature Geoscience*, 4(10), 717–722.
622 <https://doi.org/10.1038/ngeo1265>
- 623 Fernández, C., Fariás, L., & Alcaman, M. E. (2009). Primary production and nitrogen regeneration processes in
624 surface waters of the Peruvian upwelling system. *Progress in Oceanography*, 83(1–4), 159–168.
625 <https://doi.org/10.1016/j.pocean.2009.07.010>
- 626 Flynn, K. (1999). Nitrate transport and ammonium-nitrate interactions at high nitrate concentrations and low
627 temperature. *Marine Ecology Progress Series*, 187, 283–287. <https://doi.org/10.3354/meps187283>
- 628 Follows, M. J., Dutkiewicz, S., Grant, S., & Chisholm, S. W. (2007). Emergent Biogeography of Microbial
629 Communities in a Model Ocean. *Science*, 315(5820), 1843–1846. <https://doi.org/10.1126/science.1138544>
- 630 Garcia, H. E., Weathers, K. W., Paver, C. R., Smolyar, I., Boyer, T. P., Locarnini, R. A., et al. (2019). *World Ocean*
631 *Atlas 2018. Volume 4 : Dissolved Inorganic Nutrients (phosphate, nitrate and nitrate+nitrite, silicate)*. (A. M.
632 T. Editor, Ed.), *NOAA Atlas NESDIS 84* (Vol. 2).
- 633 Glibert, P. M., Wilkerson, F. P., Dugdale, R. C., Raven, J. A., Dupont, C. L., Leavitt, P. R., et al. (2016). Pluses and
634 minuses of ammonium and nitrate uptake and assimilation by phytoplankton and implications for productivity
635 and community composition, with emphasis on nitrogen-enriched conditions. *Limnology and Oceanography*,
636 61(1), 165–197. <https://doi.org/10.1002/lno.10203>
- 637 Herrero, A., Muro-Pastor, A. M., & Flores, E. (2001). Nitrogen Control in Cyanobacteria. *Journal of Bacteriology*,
638 183(2), 411–425. <https://doi.org/10.1128/JB.183.2.411-425.2001>
- 639 Horak, R. E. A., Qin, W., Schauer, A. J., Armbrust, E. V., Ingalls, A. E., Moffett, J. W., et al. (2013). Ammonia
640 oxidation kinetics and temperature sensitivity of a natural marine community dominated by Archaea. *The*
641 *ISME Journal*, 7(10), 2023–2033. <https://doi.org/10.1038/ismej.2013.75>
- 642 Huesemann, M. H., Skillman, A. D., & Crecelius, E. A. (2002). The inhibition of marine nitrification by ocean
643 disposal of carbon dioxide. *Marine Pollution Bulletin*, 44(2), 142–148. [https://doi.org/10.1016/S0025-326X\(01\)00194-1](https://doi.org/10.1016/S0025-326X(01)00194-1)
- 644 Ibarbalz, F. M., Henry, N., Brandão, M. C., Martini, S., Busseni, G., Byrne, H., et al. (2019). Global Trends in
645 Marine Plankton Diversity across Kingdoms of Life. *Cell*, 179(5), 1084–1097.e21.
646 <https://doi.org/10.1016/j.cell.2019.10.008>
- 647 Joubert, W. R., Thomalla, S. J., Waldron, H. N., Lucas, M. I., Boye, M., Le Moigne, F. A. C., et al. (2011). Nitrogen
648 uptake by phytoplankton in the Atlantic sector of the Southern Ocean during late austral summer.
649 *Biogeosciences*, 8(10), 2947–2959. <https://doi.org/10.5194/bg-8-2947-2011>
- 650 Kitidis, V., Laverock, B., McNeill, L. C., Beesley, A., Cummings, D., Tait, K., et al. (2011). Impact of ocean
651 acidification on benthic and water column ammonia oxidation. *Geophysical Research Letters*, 38(21), n/a-n/a.
652 <https://doi.org/10.1029/2011GL049095>
- 653 Klawonn, I., Bonaglia, S., Whitehouse, M. J., Littmann, S., Tienken, D., Kuypers, M. M. M., et al. (2019).
654 Untangling hidden nutrient dynamics: rapid ammonium cycling and single-cell ammonium assimilation in
655 marine plankton communities. *The ISME Journal*, 13(8), 1960–1974. <https://doi.org/10.1038/s41396-019-0386-z>
- 656 Kraft, B., Jehmlich, N., Larsen, M., Bristow, L. A., Könneke, M., Thamdrup, B., & Canfield, D. E. (2022). Oxygen
657 and nitrogen production by an ammonia-oxidizing archaeon. *Science*, 375(6576), 97–100.
658 <https://doi.org/10.1126/science.abe6733>
- 659 Krumhardt, K. M., Long, M. C., Sylvester, Z. T., & Petrik, C. M. (2022). Climate drivers of Southern Ocean
660 phytoplankton community composition and potential impacts on higher trophic levels. *Frontiers in Marine*
661 *Science*, 9. <https://doi.org/10.3389/fmars.2022.916140>
- 662 Lampe, R. H., Mann, E. L., Cohen, N. R., Till, C. P., Thamatrakoln, K., Brzezinski, M. A., et al. (2018). Different
663 iron storage strategies among bloom-forming diatoms. *Proceedings of the National Academy of Sciences*,
664 115(52), E12275–E12284. <https://doi.org/10.1073/pnas.1805243115>
- 665 Leblanc, K., Quéguiner, B., Diaz, F., Cornet, V., Michel-Rodriguez, M., Durrieu de Madron, X., et al. (2018).
666 Nanoplanktonic diatoms are globally overlooked but play a role in spring blooms and carbon export. *Nature*
667 *Communications*, 9(1), 953. <https://doi.org/10.1038/s41467-018-03376-9>
- 668 Legendre, L. (1990). The significance of microalgal blooms for fisheries and for the export of particulate organic
669 carbon in oceans. *Journal of Plankton Research*, 12(4), 681–699. <https://doi.org/10.1093/plankt/12.4.681>
- 670 Litchman, E. (2007). Resource Competition and the Ecological Success of Phytoplankton. In *Evolution of Primary*
671 *Producers in the Sea* (pp. 351–375). Elsevier. <https://doi.org/10.1016/B978-012370518-1/50017-5>

- 674 Litchman, E., Klausmeier, C. A., Schofield, O. M., & Falkowski, P. G. (2007). The role of functional traits and
675 trade-offs in structuring phytoplankton communities: scaling from cellular to ecosystem level. *Ecology*
676 *Letters*, 10(12), 1170–1181. <https://doi.org/10.1111/j.1461-0248.2007.01117.x>
- 677 Llort, J., Lévy, M., Sallée, J. B., & Tagliabue, A. (2019). Nonmonotonic Response of Primary Production and
678 Export to Changes in Mixed-Layer Depth in the Southern Ocean. *Geophysical Research Letters*, (2017),
679 2018GL081788. <https://doi.org/10.1029/2018GL081788>
- 680 Margalef, R. (1978). Life-forms of phytoplankton as survival alternatives in an unstable environment. *Oceanologica*
681 *Acta*, 1(4), 493–509.
- 682 Martens-Habbena, W., Berube, P. M., Urakawa, H., de la Torre, J. R., & Stahl, D. A. (2009). Ammonia oxidation
683 kinetics determine niche separation of nitrifying Archaea and Bacteria. *Nature*, 461(7266), 976–979.
684 <https://doi.org/10.1038/nature08465>
- 685 Matsumoto, K., Abe, O., Fujiki, T., Sukigara, C., & Mino, Y. (2016). Primary productivity at the time-series stations
686 in the northwestern Pacific Ocean: is the subtropical station unproductive? *Journal of Oceanography*, 72(3),
687 359–371. <https://doi.org/10.1007/s10872-016-0354-4>
- 688 Mduyana, M., Thomalla, S. J., Philibert, R., Ward, B. B., & Fawcett, S. E. (2020). The Seasonal Cycle of Nitrogen
689 Uptake and Nitrification in the Atlantic Sector of the Southern Ocean. *Global Biogeochemical Cycles*, 34(7),
690 1–29. <https://doi.org/10.1029/2019GB006363>
- 691 Merbt, S. N., Stahl, D. A., Casamayor, E. O., Marti, E., Nicol, G. W., & Prosser, J. I. (2012). Differential
692 photoinhibition of bacterial and archaeal ammonia oxidation. *FEMS Microbiology Letters*, 327(1), 41–46.
693 <https://doi.org/10.1111/j.1574-6968.2011.02457.x>
- 694 Metzler, P. M., Glibert, P. M., Gaeta, S. A., & Ludlam, J. M. (1997). New and regenerated production in the South
695 Atlantic off Brazil. *Deep Sea Research Part I: Oceanographic Research Papers*, 44(3), 363–384.
696 [https://doi.org/10.1016/S0967-0637\(96\)00129-X](https://doi.org/10.1016/S0967-0637(96)00129-X)
- 697 Morando, M., & Capone, D. G. (2018). Direct utilization of organic nitrogen by phytoplankton and its role in
698 nitrogen cycling within the southern California bight. *Frontiers in Microbiology*, 9(SEP).
699 <https://doi.org/10.3389/fmicb.2018.02118>
- 700 Newell, S. E., Fawcett, S. E., & Ward, B. B. (2013). Depth distribution of ammonia oxidation rates and ammonia-
701 oxidizer community composition in the Sargasso Sea. *Limnology and Oceanography*, 58(4), 1491–1500.
702 <https://doi.org/10.4319/lo.2013.58.4.1491>
- 703 Olson, R. J. (1981). Differential photoinhibition of marine nitrifying bacteria: a possible mechanism for the
704 formation of the primary nitrite maximum. *Journal of Marine Research*, 39, 227–238.
- 705 Van Oostende, N., Fawcett, S. E., Marconi, D., Lueders-Dumont, J., Sabadel, A. J. M., Woodward, E. M. S., et al.
706 (2017). Variation of summer phytoplankton community composition and its relationship to nitrate and
707 regenerated nitrogen assimilation across the North Atlantic Ocean. *Deep Sea Research Part I: Oceanographic*
708 *Research Papers*, 121(November 2016), 79–94. <https://doi.org/10.1016/j.dsr.2016.12.012>
- 709 Parker, M. S., & Armbrust, E. V. (2005). Synergistic effects of light, temperature, and nitrogen source on
710 transcription of genes for carbon and nitrogen metabolism in the centric diatom *Thalassiosira Pseudonana*
711 (*Bacillariophyceae*). *Journal of Phycology*, 41(6), 1142–1153. [https://doi.org/10.1111/j.1529-](https://doi.org/10.1111/j.1529-8817.2005.00139.x)
712 [8817.2005.00139.x](https://doi.org/10.1111/j.1529-8817.2005.00139.x)
- 713 Peng, X., Fuchsman, C. A., Jayakumar, A., Warner, M. J., Devol, A. H., & Ward, B. B. (2016). Revisiting
714 nitrification in the Eastern Tropical South Pacific: A focus on controls. *Journal of Geophysical Research:*
715 *Oceans*, 121(3), 1667–1684. <https://doi.org/10.1002/2015JC011455>
- 716 Philibert, M. C. R. (2015). *A comparative study of nitrogen uptake and nitrification rates in sub-tropical, polar and*
717 *upwelling waters*. University of Cape Town. Retrieved from <http://hdl.handle.net/11427/16794>
- 718 Pierella Karlusich, J. J., Ibarbalz, F. M., & Bowler, C. (2020). Phytoplankton in the Tara Ocean. *Annual Review of*
719 *Marine Science*, 12(1), 233–265. <https://doi.org/10.1146/annurev-marine-010419-010706>
- 720 Pierella Karlusich, J. J., Pelletier, E., Zinger, L., Lombard, F., Zingone, A., Colin, S., et al. (2022). A robust
721 approach to estimate relative phytoplankton cell abundances from metagenomes. *Molecular Ecology*
722 *Resources*. <https://doi.org/10.1111/1755-0998.13592>
- 723 Qin, W., Carlson, L. T., Armbrust, E. V., Devol, A. H., Moffett, J. W., Stahl, D. A., & Ingalls, A. E. (2015).
724 Confounding effects of oxygen and temperature on the TEX 86 signature of marine Thaumarchaeota.
725 *Proceedings of the National Academy of Sciences*, 112(35), 10979–10984.
726 <https://doi.org/10.1073/pnas.1501568112>
- 727 Raes, E. J., van de Kamp, J., Bodrossy, L., Fong, A. A., Riekenberg, J., Holmes, B. H., et al. (2020). N₂ Fixation
728 and New Insights Into Nitrification From the Ice-Edge to the Equator in the South Pacific Ocean. *Frontiers in*
729 *Marine Science*, 7(May), 1–20. <https://doi.org/10.3389/fmars.2020.00389>

- 730 Raimbault, P., Slawyk, G., Boudjellal, B., Coatanoan, C., Conan, P., Coste, B., et al. (1999). Carbon and nitrogen
731 uptake and export in the equatorial Pacific at 150°W: Evidence of an efficient regenerated production cycle.
732 *Journal of Geophysical Research: Oceans*, 104(C2), 3341–3356. <https://doi.org/10.1029/1998JC900004>
- 733 Rees, A. P., Woodward, E. M. S., & Joint, I. (2006). Concentrations and uptake of nitrate and ammonium in the
734 Atlantic Ocean between 60°N and 50°S. *Deep Sea Research Part II: Topical Studies in Oceanography*,
735 53(14–16), 1649–1665. <https://doi.org/10.1016/j.dsr2.2006.05.008>
- 736 Riahi, K., Rao, S., Krey, V., Cho, C., Chirkov, V., Fischer, G., et al. (2011). RCP 8.5—A scenario of comparatively
737 high greenhouse gas emissions. *Climatic Change*, 109(1–2), 33–57. <https://doi.org/10.1007/s10584-011-0149->
738 [y](https://doi.org/10.1007/s10584-011-0149-y)
- 739 Riahi, K., van Vuuren, D. P., Kriegler, E., Edmonds, J., O'Neill, B. C., Fujimori, S., et al. (2017). The Shared
740 Socioeconomic Pathways and their energy, land use, and greenhouse gas emissions implications: An
741 overview. *Global Environmental Change*, 42, 153–168. <https://doi.org/10.1016/j.gloenvcha.2016.05.009>
- 742 Rii, Y., Karl, D., & Church, M. (2016). Temporal and vertical variability in picophytoplankton primary productivity
743 in the North Pacific Subtropical Gyre. *Marine Ecology Progress Series*, 562, 1–18.
744 <https://doi.org/10.3354/meps11954>
- 745 Ryan-Keogh, T. J., Thomalla, S. J., Monteiro, P. M. S., & Tagliabue, A. (2023). Multidecadal trend of increasing
746 iron stress in Southern Ocean phytoplankton. *Science*, 379(6634), 834–840.
747 <https://doi.org/10.1126/science.abl5237>
- 748 Sallée, J., Pellichero, V., Akhoudas, C., Pauthenet, E., Vignes, L., Schmidtko, S., et al. (2021). Summertime
749 increases in upper-ocean stratification and mixed-layer depth. *Nature*, 591(7851), 592–598.
750 <https://doi.org/10.1038/s41586-021-03303-x>
- 751 Santoro, A. E., Sakamoto, C. M., Smith, J. M., Plant, J. N., Gehman, A. L., Worden, A. Z., et al. (2013).
752 Measurements of nitrite production in and around the primary nitrite maximum in the central California
753 Current. *Biogeosciences*, 10(11), 7395–7410. <https://doi.org/10.5194/bg-10-7395-2013>
- 754 Santoro, Alyson E., Buchwald, C., Knapp, A. N., Berelson, W. M., Capone, D. G., & Casciotti, K. L. (2021).
755 Nitrification and Nitrous Oxide Production in the Offshore Waters of the Eastern Tropical South Pacific.
756 *Global Biogeochemical Cycles*, 35(2), 1–21. <https://doi.org/10.1029/2020GB006716>
- 757 Selph, K. E., Swalethorp, R., Stukel, M. R., Kelly, T. B., Knapp, A. N., Fleming, K., et al. (2021). Phytoplankton
758 community composition and biomass in the oligotrophic Gulf of Mexico. *Journal of Plankton Research*, 1–20.
759 <https://doi.org/10.1093/plankt/fbab006>
- 760 Shafiee, R. T., Snow, J. T., Zhang, Q., & Rickaby, R. E. M. (2019). Iron requirements and uptake strategies of the
761 globally abundant marine ammonia-oxidising archaeon, *Nitrosopumilus maritimus* SCM1. *The ISME Journal*.
762 <https://doi.org/10.1038/s41396-019-0434-8>
- 763 Shiozaki, T., Ijichi, M., Isobe, K., Hashihama, F., Nakamura, K., Ehama, M., et al. (2016). Nitrification and its
764 influence on biogeochemical cycles from the equatorial Pacific to the Arctic Ocean. *The ISME Journal*, 10(9),
765 2184–2197. <https://doi.org/10.1038/ismej.2016.18>
- 766 Sommer, U., Stibor, H., Katechakis, A., Sommer, F., & Hansen, T. (2002). Pelagic food web configurations at
767 different levels of nutrient richness and their implications for the ratio fish production:primary production.
768 *Hydrobiologia*, 484, 11–20. <https://doi.org/10.1023/A:1021340601986>
- 769 Spieck, E., & Lipski, A. (2011). Cultivation, Growth Physiology, and Chemotaxonomy of Nitrite-Oxidizing
770 Bacteria. In *Methods in Enzymology* (1st ed., Vol. 486, pp. 109–130). Elsevier Inc.
771 <https://doi.org/10.1016/B978-0-12-381294-0.00005-5>
- 772 Sugie, K., Fujiwara, A., Nishino, S., Kameyama, S., & Harada, N. (2020). Impacts of Temperature, CO₂, and
773 Salinity on Phytoplankton Community Composition in the Western Arctic Ocean. *Frontiers in Marine*
774 *Science*, 6. <https://doi.org/10.3389/fmars.2019.00821>
- 775 Tagliabue, A., Aumont, O., DeAth, R., Dunne, J. P., Dutkiewicz, S., Galbraith, E., et al. (2016). How well do global
776 ocean biogeochemistry models simulate dissolved iron distributions? *Global Biogeochemical Cycles*, 30(2),
777 149–174. <https://doi.org/10.1002/2015GB005289>
- 778 Taucher, J., Bach, L. T., Prowe, A. E. F., Boxhammer, T., Kvale, K., & Riebesell, U. (2022). Enhanced silica export
779 in a future ocean triggers global diatom decline. *Nature*, 605(7911), 696–700. <https://doi.org/10.1038/s41586->
780 [022-04687-0](https://doi.org/10.1038/s41586-022-04687-0)
- 781 Thomalla, S. J., Waldron, H. N., Lucas, M. I., Read, J. F., Anson, I. J., & Pakhomov, E. (2011). Phytoplankton
782 distribution and nitrogen dynamics in the southwest Indian subtropical gyre and Southern Ocean waters.
783 *Ocean Science*, 7(1), 113–127. <https://doi.org/10.5194/os-7-113-2011>

- 784 Tolar, B. B., Ross, M. J., Wallsgrove, N. J., Liu, Q., Aluwihare, L. I., Popp, B. N., & Hollibaugh, J. T. (2016).
785 Contribution of ammonia oxidation to chemoautotrophy in Antarctic coastal waters. *The ISME Journal*,
786 *10*(11), 2605–2619. <https://doi.org/10.1038/ismej.2016.61>
- 787 Tréguer, P., Bowler, C., Moriceau, B., Dutkiewicz, S., Gehlen, M., Aumont, O., et al. (2018). Influence of diatom
788 diversity on the ocean biological carbon pump. *Nature Geoscience*, *11*(1), 27–37.
789 <https://doi.org/10.1038/s41561-017-0028-x>
- 790 Tungaraza, C., Rousseau, V., Brion, N., Lancelot, C., Gichuki, J., Baeyens, W., & Goeyens, L. (2003). Contrasting
791 nitrogen uptake by diatom and Phaeocystis-dominated phytoplankton assemblages in the North Sea. *Journal*
792 *of Experimental Marine Biology and Ecology*, *292*(1), 19–41. [https://doi.org/10.1016/S0022-0981\(03\)00145-](https://doi.org/10.1016/S0022-0981(03)00145-X)
793 [X](https://doi.org/10.1016/S0022-0981(03)00145-X)
- 794 Uitz, J., Claustre, H., Gentili, B., & Stramski, D. (2010). Phytoplankton class-specific primary production in the
795 world's oceans: Seasonal and interannual variability from satellite observations. *Global Biogeochemical*
796 *Cycles*, *24*(3), n/a-n/a. <https://doi.org/10.1029/2009GB003680>
- 797 Vannier, T., Leconte, J., Seeleuthner, Y., Mondy, S., Pelletier, E., Aury, J.-M., et al. (2016). Survey of the green
798 picoalga *Bathycoccus* genomes in the global ocean. *Scientific Reports*, *6*(1), 37900.
799 <https://doi.org/10.1038/srep37900>
- 800 de Vargas, C., Audic, S., Henry, N., Decelle, J., Mahé, F., Logares, R., et al. (2015). Eukaryotic plankton diversity
801 in the sunlit ocean. *Science*, *348*(6237). <https://doi.org/10.1126/science.1261605>
- 802 Wan, Xianhui S., Sheng, H., Dai, M., Church, M. J., Zou, W., Li, X., et al. (2021). Phytoplankton-Nitrifier
803 Interactions Control the Geographic Distribution of Nitrite in the Upper Ocean. *Global Biogeochemical*
804 *Cycles*, *35*(11), 1–19. <https://doi.org/10.1029/2021GB007072>
- 805 Wan, Xianhui Sean, Sheng, H.-X., Dai, M., Zhang, Y., Shi, D., Trull, T. W., et al. (2018). Ambient nitrate switches
806 the ammonium consumption pathway in the euphotic ocean. *Nature Communications*, *9*(1), 915.
807 <https://doi.org/10.1038/s41467-018-03363-0>
- 808 Ward, B. B. (1987). Kinetic studies on ammonia and methane oxidation by *Nitrosococcus oceanus*. *Archives of*
809 *Microbiology*, *147*(2), 126–133. <https://doi.org/10.1007/BF00415273>
- 810 Whitt, D. B., & Jansen, M. F. (2020). Slower nutrient stream suppresses Subarctic Atlantic Ocean biological
811 productivity in global warming. *Proceedings of the National Academy of Sciences*, *117*(27), 15504–15510.
812 <https://doi.org/10.1073/pnas.2000851117>
- 813 Wood, S. N. (2006). *Generalized Additive Models*. Chapman and Hall/CRC. <https://doi.org/10.1201/9781420010404>
- 814 Yang, B., Emerson, S. R., & Quay, P. D. (2019). The Subtropical Ocean's Biological Carbon Pump Determined
815 From O₂ and DIC/DI₁₃ C Tracers. *Geophysical Research Letters*, *46*(10), 5361–5368.
816 <https://doi.org/10.1029/2018GL081239>
- 817 Yingling, N., Kelly, T. B., Shropshire, T. A., Landry, M. R., Selph, K. E., Knapp, A. N., et al. (2021). Taxon-
818 specific phytoplankton growth, nutrient utilization and light limitation in the oligotrophic Gulf of Mexico.
819 *Journal of Plankton Research*, 1–21. <https://doi.org/10.1093/plankt/fbab028>
- 820 Zakem, E. J., Al-Haj, A., Church, M. J., Van Dijken, G. L., Dutkiewicz, S., Foster, S. Q., et al. (2018). Ecological
821 control of nitrite in the upper ocean. *Nature Communications*, *9*(1). [https://doi.org/10.1038/s41467-018-](https://doi.org/10.1038/s41467-018-03553-w)
822 [03553-w](https://doi.org/10.1038/s41467-018-03553-w)
- 823 Zeebe, R. E., & Wolf-Gladrow, D. A. (2001). *CO₂ in seawater: equilibrium, kinetics, isotopes* (65th ed.). Gulf
824 Professional Publishing.
- 825

